Anais XIV Simpósio Brasileiro de Sensoriamento Remoto, Natal, Brasil, 25-30 abril 2009, INPE, p. 6393-6399.

On the propagation of the Upper Ocean Heat Anomalies in the South Atlantic

Wilton Zumpichiatti Arruda
Universidade Federal do Rio de Janeiro (UFRJ) – Instituto de Matemática
Ilha do Fundão, C.P. 68530 - 21945-970 - Rio de Janeiro – RJ, Brasil
wilton@im.ufrj.br

Carlos Alessandre Domingos Lentini
Universidade Federal da Bahia (UFBA) – Instituto de Física
Travessa Barão de Jeremoabo, s/n, Campus Ondina, Salvador - BA, Brasil
clentini@ufba.br

Abstract. Using remote sensed sea high anomalies and sea surface temperature, as well as climatological temperature and salinity data in conjunction with a regional reduced gravity model, maps of Upper Layer Heat Content (ULH) for the South Atlantic are generated. Prior to the computations of the ULH anomalies (ULHAs), the estimated seasonal cycle is calculated and then subtracted to the ULH maps. In order to study the propagation of ULHAs, Hovmöller diagrams at 25.5°S, 30.5°S, and along South American coast between 25.5°S and 36.5°S are plotted. Using visual inspection and two-dimensional spectrum technique on the Hovmöller diagrams we show that the ULHAs propagate westward with a period of 4.63 years in the Subtropical region with phase speed comparable to long first mode baroclinic Rossby waves. As they reach the South American East coast the ULHAs are advected southward by the Brazil Current (BC). We speculate the southward advection of these anomalies is probably related to the variability in the BC transport: advection of positive (negative) ULHAs is associated with an increase (decrease) in the BC transport. Moreover, the ULHAs advected by the BC accumulate in the Brazil-Malvinas confluence. The release of ULH excess (deficit) would be achieved through the shedding of anticyclonic (cyclonic) warm (cold) core eddies in the confluence region during a “warm” (“cold”) event.

Keywords: SHA, SST, upper layer, heat content, Brazil-Malvinas confluence, warm core eddies, cold core eddies, South Atlantic, two-dimensional spectrum.

Palavras chave: SHA, TSM, camada superior, conteúdo de calor, Confluência Brasil-Malvinas, vórtices de núcleos quentes, vórtices de núcleos frios, espectro bi-dimensional.

1. Introduction

The lack of continuous long-term hydrographic observations makes satellite-derived data an extremely useful tool to investigate time and spatial variability of ocean basins such as the South Atlantic. Unlike infrared imagery, which only reflects the thermal conditions in a very thin layer of the sea surface, altimeter signals are unaffected by cloud coverage and provide information on the vertical thermal and dynamical structure of the upper ocean when complemented by climatological hydrographic data within a regional diagnostic model (Goni et al., 1996, 1997; Garzoli and Goni 2000; Arruda et al., 2005; Lentini et al., 2006).

Current research and operational global atmosphere and ocean models rely on satellite-based data for forecasting purposes and studies on climate variability. In fact, one of the main goals of climate research is the prediction of relative long term changes in global climate. Due to the ocean's high thermal inertia it is believed that the Earth's climate is adjusted by the ocean's troposphere, where heat fluxes play a vital role on air-sea process. Therefore, the understanding of how the amount of heat stored in the ocean’s upper layer varies is crucial.

Gordon (1986) in his famous paper about the “Great Conveyor Belt” suggests that the flow of the North Atlantic Deep Water (NADW) from North to South Atlantic and its later spreading into the Pacific and Indian Oceans should be balanced by a thermocline return flow. In the South Atlantic the return flow has two possible components. The so-called warm water route, which brings warm salty waters from the Indian Ocean to the Southwestern Atlantic via the Agulhas Leakage, and the so-called cold water route, which brings cold intermediate waters from the Pacific Ocean to the Southeastern Atlantic via the Drake Passage. Gordon (1986) suggests that the warm water route is the most important source for the return flow in the South Atlantic, although this controversy is not clear yet (Ruijter et al., 1999). The influx of warm salty waters from the Indian Ocean is mostly due to eddy shedding from the Agulhas Retroflection and Benguela Current (Gordon, 1986; Ruijter et al. 1999, Goni et al, 1997; Garzoli et al., 1999). The injection of warm waters into the Southwestern South Atlantic is responsible for its unique characteristic in the net heat flux: the net flux of heat toward and across the equator.

Therefore, the objective of this work is to use the satellite-derived upper ocean heat content to study the propagation of upper ocean heat anomalies in the South Atlantic.

2. Data and Methods

Both altimeter and sea surface temperature datasets have the same spatial resolution (1^o x 1^o) with all missing data filled in by an optimal interpolation scheme. For further information, the product documentation is at http://podaac.jpl.nasa.gov/products. The World Ocean Atlas 2001 hydrographic data (WOA01) is obtained at the http://www.nodc.noaa.gov site. This dataset contains temperature and salinity values at standard levels with the same grid as the satellite data.

TOPEX/POSEIDON (T/P) Sea Surface Height Anomalies (SHA) for the period from October 1992 to December 2001, averaged over each 5 days and referenced to the 1993-2001 mean with tidal and inverted barometer effects removed, are used here.

PATHFINDER AVHRR Sea Surface Temperature (SST) V4.1 data for January 1990 to December 2001, averaged also over each 5 days, using version 4.1 is also used.

For our purposes, we assume that the ocean can be approximated by a regional reduced gravity model. In this model, only the top layer is active, while the bottom layer is assumed to be infinite deep and motionless. Therefore, the upper layer thickness can be estimated as,

$$h(x,y,t) = \bar{h}(x,y) + \frac{g}{g'(x,y)}\eta'(x,y,t) \qquad (1)$$

where the h is the Upper Layer Thickness (ULT), $\bar{h}$ is the mean climatological ULT, g is the gravity, and g' the climatological reduced gravity.

Temperature and salinity data extracted from WOA01 are used to compute the climatological mean ULT ($\bar{h}$) for the region of study, which extends from the surface to the depth of the 10^oC isotherm, and the reduced gravity. According to Goni et al. (1996) the 10^oC isotherm is a good proxy to define the lower subsurface limit of the South Atlantic Thermocline Water (SATW) in the subtropical gyre. The lower layer is defined as the layer between the depth of the 10^oC isotherm and 1500 m. These climatologically-derived values are then used in conjunction with (1) to generate the ULT maps.

The Upper Layer Heat Content (ULH) in the upper layer is defined as,

$$\mathrm{UHC}(x,y,t) = \rho_0 C_p \int_{h(x,y,t)}^{0} \mathrm{T}(x,y,z,t)\,dz \,, \qquad (2)$$

where ρ_0 is the mean density of seawater and C_p is the specific heat of seawater, and T is temperature in degrees Kelvin.

According to Arruda et al. (2005) the integral in (2) is calculated from AVHRR-SST and linear regression coefficients between the climatological SST and the climatological mean upper layer temperature in the subtropical South Atlantic region (38.5ºS-18.5ºS,60.5ºW-20.5ºE).

In this way, the ULH is derived from the T/P-SHA and AVHRR-SST by,

$$\mathrm{ULH}(x,y,t) = \rho_0 C_p (\alpha_1 \mathrm{SST}(x,y,t) + \alpha_o) h(x,y,t), \quad (3)$$

where α_0 and α_1 the linear regression coefficients (Arruda et al.; 2005a,b).

The Upper Ocean Heat Content Anomalies (ULHAs) are obtained subtracting from (3) the annual cycle at each grid point.

3. Results

Using (3) we generate the ULHA maps for the South Atlantic during the period from October 1992 to December 2001, at every 5 days with a 1^o x 1^o spatial resolution. This dataset is suitable for studying the way the ocean redistribute the heat stored in the thermocline during long timescales.

Three Hovmöller diagrams are shown on Fig. 1: Along the latitude of 25.5ºS (Fig. 1a), along the latitude of 30.5ºS (Fig. 1b), and following the 1500m isobath along the East coast of South America between 25.5ºS and 36.5ºS (Fig. 1c).

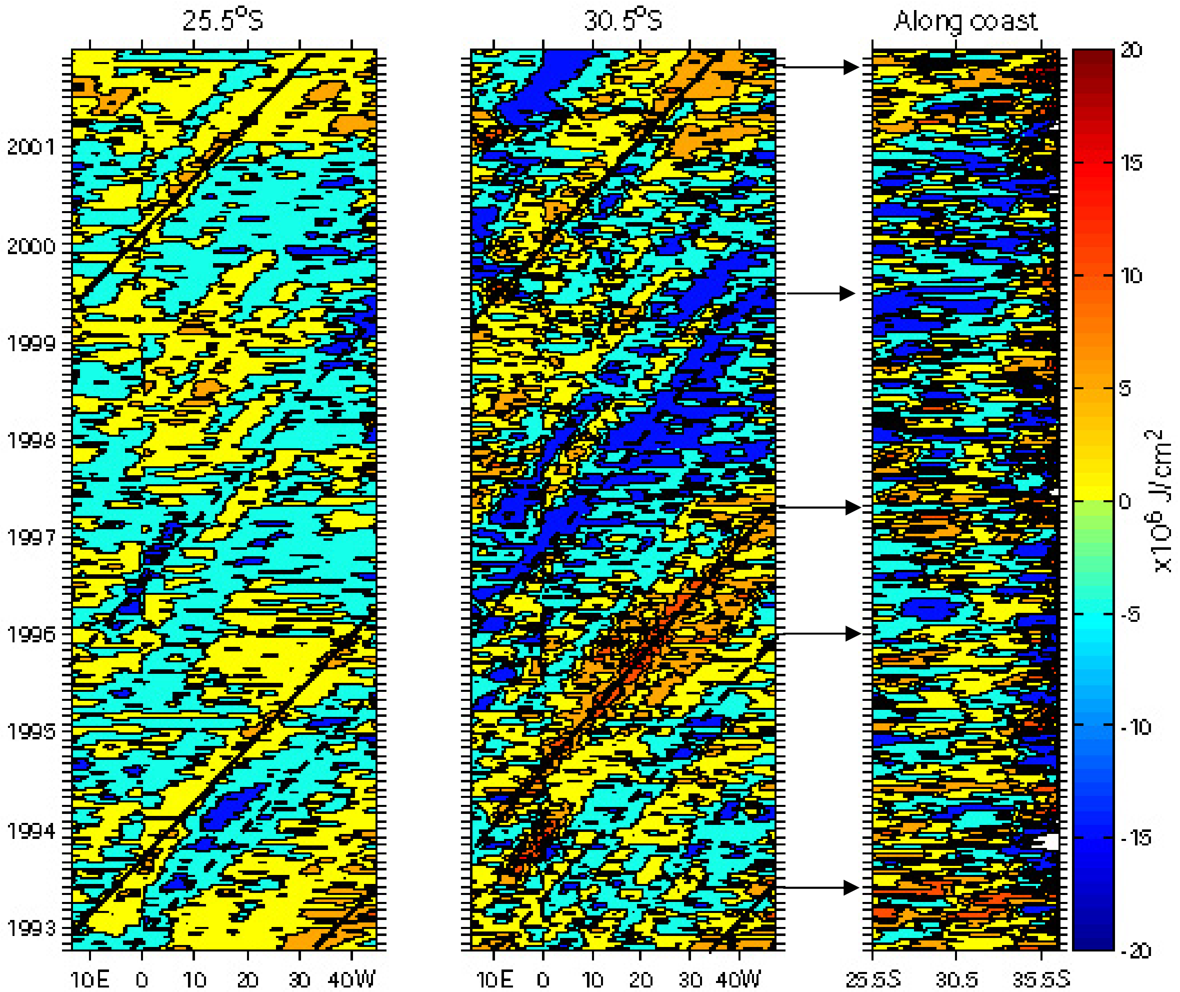

Figure 1. Hovmöller diagrams for the ULHAs (a) Along the 25.5ºS zonal section; (b) Along the 30.5ºS; (c) Along the 1500 m isobath parallel to the South American east coast between 25.5ºS and 36.5ºS. The solid lines mark the wave crests (positive ULHAs) and the dotted lines mark the wave troughs (negative ULHAs).

Along the two zonal sections at 25.5ºS the 30.5ºS (Fig. 1a,b) the most prominent features are propagating westward signals. The propagation is more evident on the 30.5ºS latitude. On both diagrams we added straight lines aligned with the propagating signals. The solid lines mark the wave crests (positive ULHAs) and the dotted lines mark the wave troughs (negative ULHAs). From the slope of each line we can estimate the wave phase speed. At 25.5ºS the signal takes about 40 months to go from 12.3ºE to 44.5ºW, what gives a phase speed of 4.7 cm/s. At 30.5ºS the signal takes about 41 months to go from 14.3ºE to 47.5ºW, what gives a phase speed of 4.8 cm/s.

As the ULHAs reach the continent it follows a southward path along the coast, as can be seen on Fig. 1c.

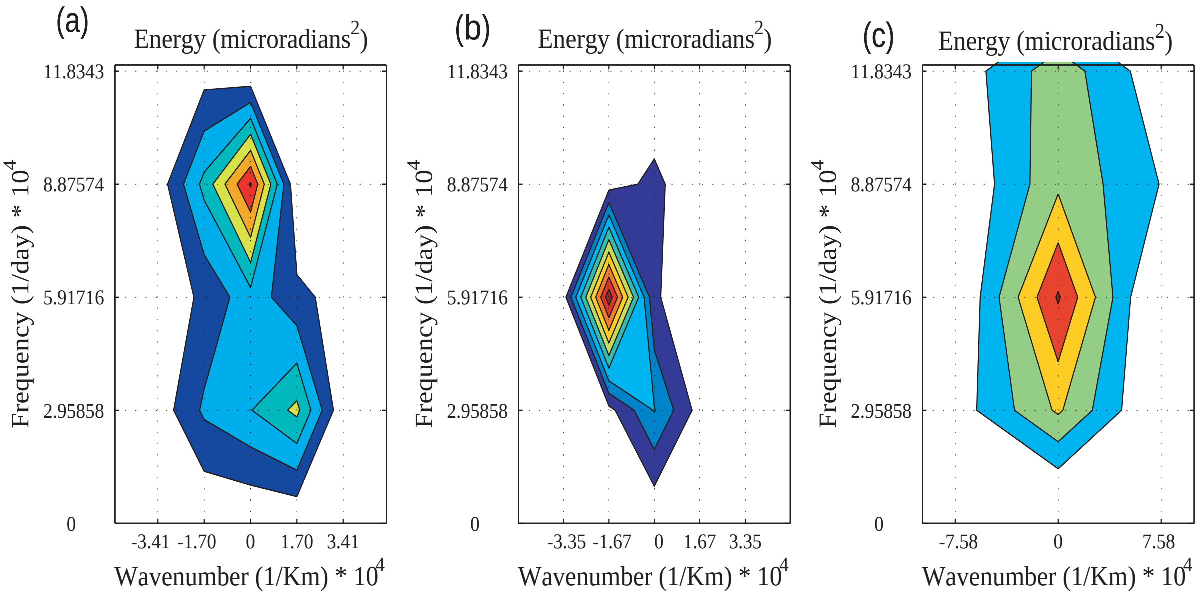

Figure 2. Two dimensional energy spectra for the Hovmöller diagrams on Fig. 1: (a) Along the 25.5ºS zonal section; (b) Along the 30.5ºS zonal section; (c) Along the 1500 m isobath parallel to the South American east coast and between 25.5ºS and 35.5ºS.

For each Hovmöller diagram on Fig.1 we calculate the two-dimensional (2-D) spectrum. The 2-D spectrum is valuable tool, since it displays wavenumer and frequency of the most energetic propagating signals on a Hovmöller diagram. A negative wavenumber means westward propagation.

At 25.5ºS (Fig. 2a) the most energetic peak has a frequency of 8.88×10^{-4} day^{-1}, what means a 3 years period. Since at this latitude the minimum wavenumber resolved is 1.7×10^{-4} km^{-1}, any wave with a wavelength larger than 5857 km will be displayed with zero wavenumber. At 30.5ºS (Fig. 2a) the most energetic peak has a frequency of 5.92×10^{-4} day^{-1} (or a period of 4.63 years) and a wavenumber of 1.67×10^{-4} km^{-1}, what means a wavelength of 5971 km and a phase speed of 4 cm/s. Note that the results derived from the 2-D spectrum match very closely the ones derived from visual inspection of the Hovmöller diagrams.

The along-coast diagram (Fig. 1c) indicates that there is, apparently, an along coast southward propagation. Moreover, we can see alternate positive and negative ULH anomalies. Comparing the diagrams of Fig. 1 we see that the ULHAs along the coastline coincide with the arrival of westward propagating signals, what make us hypothesize that the variability of the ULHAs along the South American East coast may be forced by the basin wide propagating signal. The 2-D energy spectrum for the along coast Hovmöller diagram (Fig. 2c) has a peak at zero wave number which is the same frequency and period of the 30.5ºS diagram. The zero wavenumber is due to the spectrum resolution. From Fig 1c, we can see that ULHAs take about 2 months to go from 25.5ºS to 36.5ºS, what gives a phase speed of 54 cm/s, what is comparable the Brazil Current (BC) speed of 50-60 cm/s at 25ºS (Peterson and Stramma, 1991). This make us hypothesize that the ULHAs propagate westward in the South Atlantic interior and, as they reach the South American East Coast, they are advected southward by the BC flow.

The mean first mode baroclinic Rossby radius of deformation (R_d) at 30.5ºS (Chelton et al., 1998) is 29.23 km, what gives a phase speed (βR_d^2) of 2.39 cm/s for long first mode baroclinic Rossby waves at this latitude. Our results (about 4 cm/s) are in accordance with previous works (Killworth et al. 1997; Challenor et al., 2004) which point out that the Rossby waves phase speeds computed from remote sensing data are about 2-3 times larger than predicted by linear theory at this latitude range.

Let's now address the question: What's the fate of the ULHAs that are advected southward along the South American coastline following the BC?

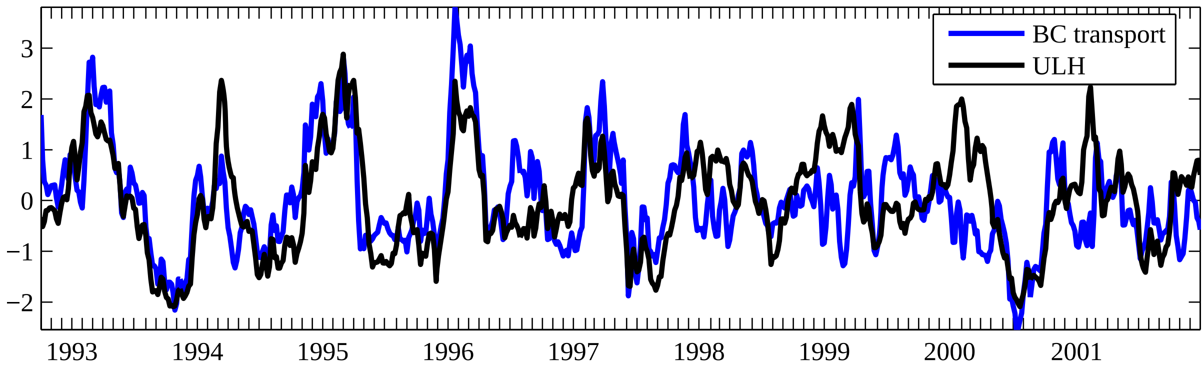

Figure 3. Blue line: Normalized BC baroclinic transport at 30.5^{o}S. Dotted line: Normalized ULH averaged over a box centered a (37.5ºS,45ºW).

Fig. 3 shows the time series of normalized BC baroclinic transport at 30.5^{o}S and normalized ULH in a region centered at (37.5ºS,45ºW). This point is inside the "pool" of positive/negative ULHA at the Brazil-Malvinas Confluence (Fig. 4). We can observe that the variability of the ULH is closely associated to the variability of the BC transport (0.76 correlation). An increase (decrease) in the BC transport is related to higher (lower) ULH at the BMC region. Therefore, the results indicate that the southward advection of ULHAs by the BC may be associated with the variability on its baroclinic transport.

Fig. 4 shows hot and cold events along the South American West coastline. It shows a distinctive wave-like pattern in the ocean interior and a uniform anomaly signal along the coastline. It is worth to observe on Fig. 4a (Fig. 4b) that there is a region of positive (negative) ULHA during the hot (cold) event at approximately 36º-45ºS and 45ºW. This indicates heat excess (deficiency) at the Brazil-Malvinas Confluence Zone.

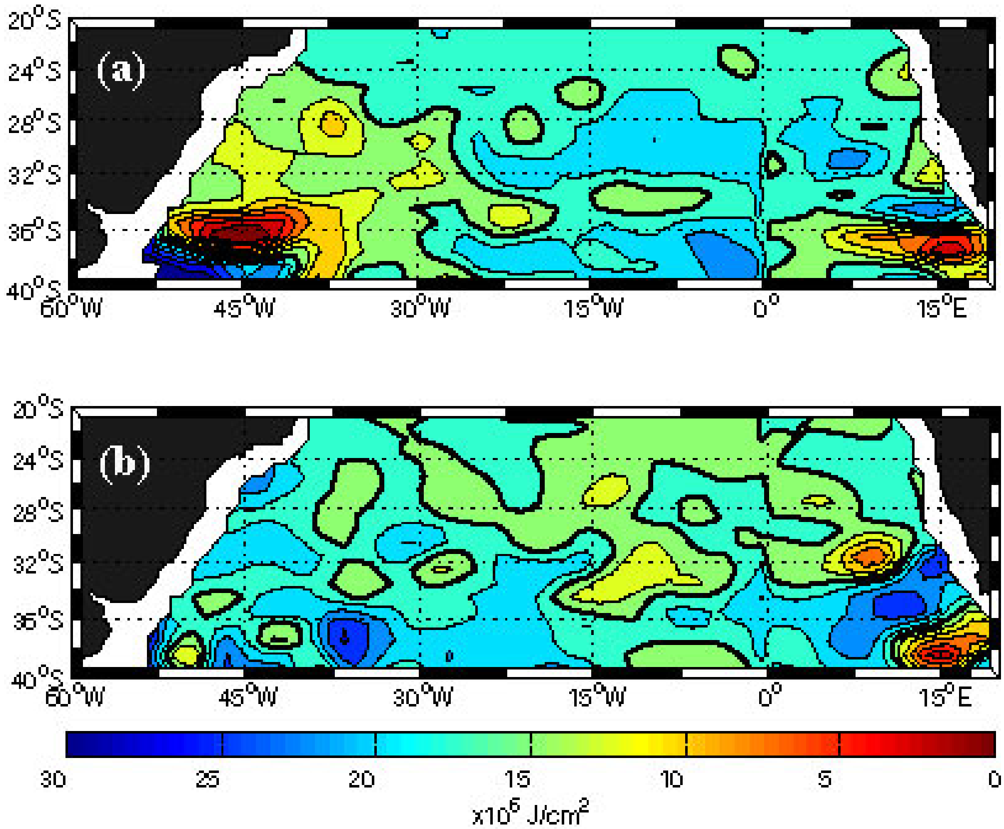

Figure 4. Upper Layer Heat Anomalies contour plots. The tick line represents the zero contour line. (a) Positive ULHA at the South Atlantic West coast for March 1997 and (b) negative ULHA at the South American coast for June 1999.

Summary and Conclusions

The results indicate that the ULHAs propagate westward from the African continent to to South America around 30.5ºS. The ULHAs propagate westward with a period of 4.63 years in the Subtropical region. The propagation phase speeds are comparable to the long first mode baroclinic Rossby waves. As they reach the South American East Coast the ULHAs follows southwestward advected by the BC. The southward advection of the ULHAs is probably related with the variability in the BC transport: Positive (negative) ULHAs advection is associated with an increase (decrease) of the BC baroclinic transport. As the ULHAs are advected southward by the BC, they accumulate in the Brazil-Malvinas Confluence Zone. According to Lentini et al. (2006): “Ring formation seems to be linked to the Brazil Current southward baroclinic transport, estimated across the T/P groundtrack d294 between 36º-38ºS, as relatively moderate-to-high increments in the upper-layer transport are usually followed by the formation and shedding of an anticyclone”. The anticyclonic warm-core eddies would then release the ULH excess accumulated in the Brazil-Malvinas Confluence Zone during a hot event to the Subtropical region. By analogy, a decrease in the BC baroclinic transport could favor the shedding of cyclonic cold-core eddies and consequent release of the ULH deficit accumulated at the Brazil-Malvinas Confluence Zone during a cold event.

Acknowledgements

The authors also would like to thank the Brazilian Research and Technology Council (CNPq) for funding the BACANA and VARICONF Projects, grants #478398/2006-9 and #476472/2006-7, respectively.

References

Arruda, W. Z., C. A. D. Lentini, and E. D. J. Campos. The use of satellite-derived upper ocean heat content to the study of climate variability in the South Atlantic. **Brazilian Journal of Cartography**., v. 57, n. 2, p. 87-92, 2005b.

Challenor, P. G.; Cipollini, P.; Cromwell, D.; Hill, K.L.; Quartly, G.D.; Robinson, I.S. Characteristics of mid-latitude Rossby wave propagation from multiple satellite datasets. **International Journal of Remote Sensing**, v. 25, n. 7-8, p. 1297-1302. 2004.

Chelton, D. B.; deSzoeke, R. A.; Schlax, M. G.; El Naggar, K. ; Siwertz, N. Geographical variability of the first-baroclinic Rossby radius of deformation. **Journal of Physical Oceanography**, v. 28, p. 433-460. 1998.

De Ruijter, W.P.M.; Biastoch, A.; Drijfhout, S.S.; Lutjeharms, J.R.E.; Matano, R.P.; Pichevin, T.; van Leeuwen, P.J.; Weijer W. Indian-Atlantic interocean exchange: Dynamics, estimation and impact. **Journal of Geophysical Research-Oceans**, v. 104**,** n. C9, 20885-20910. 1999.

Garzoli, S.L.; Richardson, P.L.; Rae, C.M.D.; Fratantoni, D.M.; Goni, G.J.; Roubicek, A.J. Three Agulhas rings observed during the Benguela Current experiment. **Journal of Geophysical Research-Oceans**, v. 104, n. C9, p. 20971-20985. 1999.

Garzoli, S.L.; Goni, G.J. Combining altimeter observations and oceanographic data for ocean circulation and climate studies. In: D. Halpern (ed.). **Satellites Oceanography and Society**, Elsevier Science, 2000. 367 p.

Goni, G. J.; Kamholz, S.; Garzoli, S.; Olson, D.B. Dynamics of the Brazil-Malvinas Confluence based on iverted echsounders and altimetry. . **Journal of Geophysical Research-Oceans**, v. 101, p. 16373-16289. 1996.

Goni, G.J.; Garzoli, S.L.; Roubicek, A.J.; Olson, D.B.; Brown, O.B. Agulhas ring dynamics from TOPEX/ POSEIDON satellite altimeter data. **Journal of Marine Research** , v. 55, n. 5, 861-883. 1997.

Horel, J.D. Complex principal component analysis: Theory and examples. **Journal of Applied Meteorology**, v. 23, n. 12, 1660–1673. 1984.

Killworth, P.D.; Chelton, D.B.; de Szoeke, R.A. The speed of observed and theoretical long extra-tropical planetary waves. **Journal of Physical Oceanography**, v. 27, 1946-1966. 1997.

Lentini, C.A.D.; G. J. Goni; Olson, D.B. Investigation of Brazil Current Rings: 1993-1998. **Journal of Geophysical Research-Oceans**, 111, C06013, doi: 10.1029/2005JC002988. 2006

Levitus, S.; Antonov, J.I.; Boyer, T.P.; Stephens, C. Warming of the world ocean. **Science**, v. 287, 2225–2229. 2000.

Merrifield, M.A.; Guza, R.T. Detecting propagating signal with Complex Empirical Orthogonal Functions: A cautionary note. **Journal of Physical Oceanography**, v. 20, 1628-1633. 1990.

Mizoguchi, K.; Meyers, S.D.; Basu, S.; O´Brien, J.J. Multi- and Quasi-Decadal Variations of Sea Surface Temperature in the North Atlantic. **Journal of Physical Oceanography**, v. 29, 3133-3144. 1999.

Peterson, R.G.; Stramma, L. Upper level circulation in the South Atlantic Ocean. **Progress in Oceanography**, v. 26, 1-73. 1991.